Supplementary File 1. The reference list related to TYMS phosphoprotein site in mammals.

[1] Very N, Hardivillé S, Decourcelle A, Thévenet J, Djouina M, Page A, Vergoten G, Schulz C, Kerr-Conte J, Lefebvre T, Dehennaut V and El Yazidi-Belkoura I. Thymidylate synthase O-GlcNAcylation: a molecular mechanism of 5-FU sensitization in colorectal cancer. Oncogene 2022; 41: 745-756.

[2] Akimov V, Barrio-Hernandez I, Hansen SVF, Hallenborg P, Pedersen AK, Bekker-Jensen DB, Puglia M, Christensen SDK, Vanselow JT, Nielsen MM, Kratchmarova I, Kelstrup CD, Olsen JV and Blagoev B. UbiSite approach for comprehensive mapping of lysine and N-terminal ubiquitination sites. Nat Struct Mol Biol 2018; 25: 631-640.

[3] Lumpkin RJ, Gu H, Zhu Y, Leonard M, Ahmad AS, Clauser KR, Meyer JG, Bennett EJ and Komives EA. Site-specific identification and quantitation of endogenous SUMO modifications under native conditions. Nat Commun 2017; 8: 1171.

[4] Mertins P, Mani DR, Ruggles KV, Gillette MA, Clauser KR, Wang P, Wang X, Qiao JW, Cao S, Petralia F, Kawaler E, Mundt F, Krug K, Tu Z, Lei JT, Gatza ML, Wilkerson M, Perou CM, Yellapantula V, Huang KL, Lin C, McLellan MD, Yan P, Davies SR, Townsend RR, Skates SJ, Wang J, Zhang B, Kinsinger CR, Mesri M, Rodriguez H, Ding L, Paulovich AG, Fenyö D, Ellis MJ and Carr SA; NCI CPTAC. Proteogenomics connects somatic mutations to signalling in breast cancer. Nature 2016; 534: 55-62.

[5] Boeing S, Williamson L, Encheva V, Gori I, Saunders RE, Instrell R, Aygün O, Rodriguez-Martinez M, Weems JC, Kelly GP, Conaway JW, Conaway RC, Stewart A, Howell M, Snijders AP and Svejstrup JQ. Multiomic analysis of the UV-Induced DNA damage response. Cell Rep 2016; 15: 1597-1610.

[6] Hendriks IA, D'Souza RC, Yang B, Verlaan-de Vries M, Mann M and Vertegaal AC. Uncovering global SUMOylation signaling networks in a site-specific manner. Nat Struct Mol Biol 2014; 21: 927-36.

[7] Mertins P, Yang F, Liu T, Mani DR, Petyuk VA, Gillette MA, Clauser KR, Qiao JW, Gritsenko MA, Moore RJ, Levine DA, Townsend R, Erdmann-Gilmore P, Snider JE, Davies SR, Ruggles KV, Fenyo D, Kitchens RT, Li S, Olvera N, Dao F, Rodriguez H, Chan DW, Liebler D, White F, Rodland KD, Mills GB, Smith RD, Paulovich AG, Ellis M and Carr SA. Ischemia in tumors induces early and sustained phosphorylation changes in stress kinase pathways but does not affect global protein levels. Mol Cell Proteomics 2014; 13: 1690-704.

[8] Tammsalu T, Matic I, Jaffray EG, Ibrahim AFM, Tatham MH and Hay RT. Proteome-wide identification of SUMO2 modification sites. Sci Signal 2014; 7: rs2.

[9] Mertins P, Qiao JW, Patel J, Udeshi ND, Clauser KR, Mani DR, Burgess MW, Gillette MA, Jaffe JD and Carr SA. Integrated proteomic analysis of post-translational modifications by serial enrichment. Nat Methods 2013; 10: 634-7.

[10] Udeshi ND, Svinkina T, Mertins P, Kuhn E, Mani DR, Qiao JW and Carr SA. Refined preparation and use of anti-diglycine remnant (K-ε-GG) antibody enables routine quantification of 10,000s of ubiquitination sites in single proteomics experiments. Mol Cell Proteomics 2013; 12: 825-31.

[11] Zhou H, Di Palma S, Preisinger C, Peng M, Polat AN, Heck AJ and Mohammed S. Toward a comprehensive characterization of a human cancer cell phosphoproteome. J Proteome Res 2013; 12: 260-71.

[12] Povlsen LK, Beli P, Wagner SA, Poulsen SL, Sylvestersen KB, Poulsen JW, Nielsen ML, Bekker-Jensen S, Mailand N and Choudhary C. Systems-wide analysis of ubiquitylation dynamics reveals a key role for PAF15 ubiquitylation in DNA-damage bypass. Nat Cell Biol 2012; 14: 1089-98.

[13] Klammer M, Kaminski M, Zedler A, Oppermann F, Blencke S, Marx S, Müller S, Tebbe A, Godl K and Schaab C. Phosphosignature predicts dasatinib response in non-small cell lung cancer. Mol Cell Proteomics 2012; 11: 651-68.

[14] Franz-Wachtel M, Eisler SA, Krug K, Wahl S, Carpy A, Nordheim A, Pfizenmaier K, Hausser A and Macek B. Global detection of protein kinase D-dependent phosphorylation events in nocodazole-treated human cells. Mol Cell Proteomics 2012; 11: 160-70.

[15] Beli P, Lukashchuk N, Wagner SA, Weinert BT, Olsen JV, Baskcomb L, Mann M, Jackson SP and Choudhary C. Proteomic investigations reveal a role for RNA processing factor THRAP3 in the DNA damage response. Mol Cell 2012; 46: 212-25.

[16] Weber C, Schreiber TB and Daub H. Dual phosphoproteomics and chemical proteomics analysis of erlotinib and gefitinib interference in acute myeloid leukemia cells. J Proteomics 2012; 75: 1343-56.

[17] Kim W, Bennett EJ, Huttlin EL, Guo A, Li J, Possemato A, Sowa ME, Rad R, Rush J, Comb MJ, Harper JW and Gygi SP. Systematic and quantitative assessment of the ubiquitin-modified proteome. Mol Cell 2011; 44: 325-40.

[18] Wagner SA, Beli P, Weinert BT, Nielsen ML, Cox J, Mann M and Choudhary C. A Proteome-wide, Quantitative survey of in vivo ubiquitylation sites reveals widespread regulatory roles. Mol Cell Proteomics 2011; 10: M111.013284.

[19] Kettenbach AN, Schweppe DK, Faherty BK, Pechenick D, Pletnev AA and Gerber SA. Quantitative phosphoproteomics identifies substrates and functional modules of aurora and polo-like kinase activities in mitotic cells. Sci Signal 2011; 4: rs5.
[20] Iliuk AB, Martin VA, Alicie BM, Geahlen RL and Tao WA. In-depth analyses of kinase-dependent tyrosine phosphoproteomes based on metal ion-functionalized soluble nanopolymers. Mol Cell Proteomics 2010; 9: 2162-72.
[21] Frączyk T, Kubiński K, Masłyk M, Cieśla J, Hellman U, Shugar D and Rode W. Phosphorylation of thymidylate synthase from various sources by human protein kinase CK2 and its catalytic subunits. Bioorg Chem 2010; 38: 124-131.
[22] Jarmuła A, Fraczyk T, Cieplak P and Rode W. Mechanism of influence of phosphorylation on serine 124 on a decrease of catalytic activity of human thymidylate synthase. Bioorg Med Chem 2010; 18: 3361-70.
[23] Olsen JV, Vermeulen M, Santamaria A, Kumar C, Miller ML, Jensen LJ, Gnad F, Cox J, Jensen TS, Nigg EA, Brunak S and Mann M. Quantitative phosphoproteomics reveals widespread full phosphorylation site occupancy during mitosis. Sci Signal 2010; 3: ra3.
[24] Jørgensen C, Sherman A, Chen GI, Pasculescu A, Poliakov A, Hsiung M, Larsen B, Wilkinson DG, Linding R and Pawson T. Cell-specific information processing in segregating populations of Eph receptor ephrin-expressing cells. Science 2009; 326: 1502-9.
[25] Choudhary C, Olsen JV, Brandts C, Cox J, Reddy PN, Böhmer FD, Gerke V, Schmidt-Arras DE, Berdel WE, Müller-Tidow C, Mann M and Serve H. Mislocalized activation of oncogenic RTKs switches downstream signaling outcomes. Mol Cell 2009; 36: 326-39.
[26] Mayya V, Lundgren DH, Hwang SI, Rezaul K, Wu L, Eng JK, Rodionov V and Han DK. Quantitative phosphoproteomic analysis of T cell receptor signaling reveals system-wide modulation of protein-protein interactions. Sci Signal 2009; 2: ra46.
[27] Anderson DD, Woeller CF and Stover PJ. Small ubiquitin-like modifier-1 (SUMO-1) modification of thymidylate synthase and dihydrofolate reductase. Clin Chem Lab Med 2007; 45: 1760-3.
[28] Rush J, Moritz A, Lee KA, Guo A, Goss VL, Spek EJ, Zhang H, Zha XM, Polakiewicz RD and Comb MJ. Immunoaffinity profiling of tyrosine phosphorylation in cancer cells. Nat Biotechnol 2005; 23: 94-101.

Supplementary Table 1. The detailed analysis of **Figure 1**

Ref. No.	Year	Journal	Summary
10	2022	JCI Insight	In Men1-mutant in vivo and in vitro background, increased levels of TYMS accelerate pancreatic neuroendocrine tumor cell proliferation, disrupt cell cycle regulation, and correlate with elevated somatic mutations, DNA damage, and genomic instability.
11	2022	Med Oncol	5-FU leads to resistance against TYMS targeting drugs. Various chemoresistance mechanisms include autophagy, apoptosis evasion, drug detoxification and altered signaling pathways containing AKT/PI3K, RAS-MAPK, WNT/β catenin, mTOR.
12	2022	Elife	E7, a novel anticancer drug, inhibits TYMS expression in both pancreatic and ovarian cancer cells and hastens its proteasomal degradation, lowering enzyme levels.
13	2022	Clin Cancer Res	Phase I clinical trials revealed CT900, a novel TYMS inhibitor targeting α-folate receptor, demonstrated an acceptable side effect profile and clinical benefit in patients with ovarian cancers.
14	2019	Cell Death Differ	In vitro, knockdown of TYMS attenuated migration and sphere formation while repressing the expression of epithelial-mesenchymal transition (EMT) signature genes. In vivo, cells deficient in TYMS demonstrated an increased ability to invade and metastasize. Mechanistically, TYMS enzymatic activity was found to be essential for maintaining the EMT/stem-like state by facilitating dihydropyrimidine dehydrogenase-dependent pyrimidine catabolism.
15	2016	Clin Cancer Res	Id1 was found to confer 5-FU chemoresistance through E2F1-dependent induction of TYMS expression in esophageal cancer. Additionally, an intricate E2F1-dependent mechanism was elucidated, whereby Id1 increases TYMS and IGF2 expressions to promote cancer chemoresistance.
16	2007	Clin Cancer Res	In NSCLC patiens, E2F1 gene expression correlates with TS gene expressions and tumor proliferation.
17	2004	Clin Cancer Res	The induction of TYMS expression inhibits Fas induction in response to raltitrexed and Alimta, leading to the inactivation of Caspase-8.
18	2004	Cancer Cell	Overexpression of TYMS results in programmed cell death following serum removal. The ectopic expression of TYMS is sufficient to induce a transformed phenotype in mammalian cells, as evidenced by foci formation, anchorage-independent growth, and tumor formation in nude mice.
19	2022	Mol Med	The MALAT1 lncRNA and miRNA (miR-197-3p, miR-203a-3p, miR-375-3p) network regulates TYMS expression and predicts chemoresistance to 5-FU treatment.
20	2022	Biomedicines	TYMS is involved in the modulation of epithelial-mesenchymal transition (EMT) and colorectal cancer metastasis. Silencing TYMS expression reverses EMT and inhibits the invasive capacity of cancer cells.
21	2014	Oncotarget	HSP90 knockdown inhibits cell cycle progression, downregulates TYMS levels, and sensitizes colorectal cancer cell lines to the effects of 5-FU.
22	2012	Aging	Simultaneous genetic inhibition of TYMS and ribonucleotide reductase in melanoma cells induces DNA damage and senescence phenotypes. Conversely, overexpression of TYMS and ribonucleotide reductase inhibits DNA damage and senescence-associated phenotypes caused by C-myc depletion.
23	2009	Int J Cancer	Histone deacetylase inhibitors (HDACi) significantly downregulate TYMS gene expression in colon cancer cell lines. This downregulation is independent of p53, p21, and HDAC2 expression and can be achieved in vivo, thereby contributing to overcoming chemoresistance to 5-FU.
24	2019	Carcino-genesis	Melatonin-mediated downregulation of thymidylate synthase as a novel mechanism for overcoming 5-fluorouracil associated chemoresistance in colorectal cancer cells.
25	2020	J Adv Res	A novel TYMS inhibitor induces apoptosis through the mitochondrial pathway in NSCLC cells by upregulating wild-type p53 protein expression. This compound also inhibits angiogenesis both in vitro and in vivo.
26	2011	J Pharmacol Exp Ther	Cisplatin increases the phosphorylation of mitogen-activated protein kinase kinase 1/2 (MKK1/2) and extracellular signal-regulated kinase 1/2 (ERK1/2), as well as the protein levels of TYMS, by enhancing protein stability in NSCLC cells. Depletion of endogenous TYMS expression significantly increases cisplatin-induced cell death and growth inhibition. Enforced expression of constitutively active MKK1/2 vectors rescues the protein levels of phospho-ERK1/2 and TYMS. In conclusion, the upregulation of ERK1/2-dependent TYMS protects NSCLC cells from cisplatin-induced cytotoxicity.

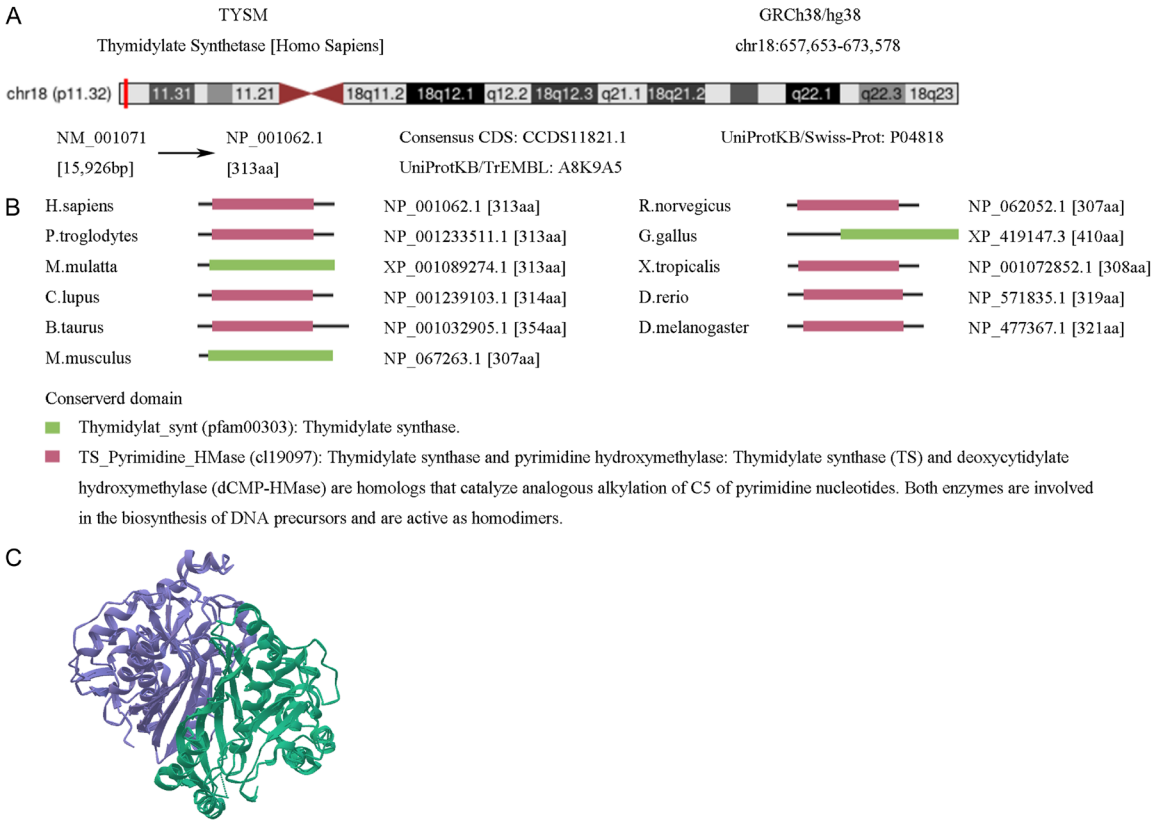

Supplementary Figure 1. Structural characteristics of TYMS. A. Gene location of TYMS. B. Conserved domain of TYMS. C. Three-dimension structure of TYMS.

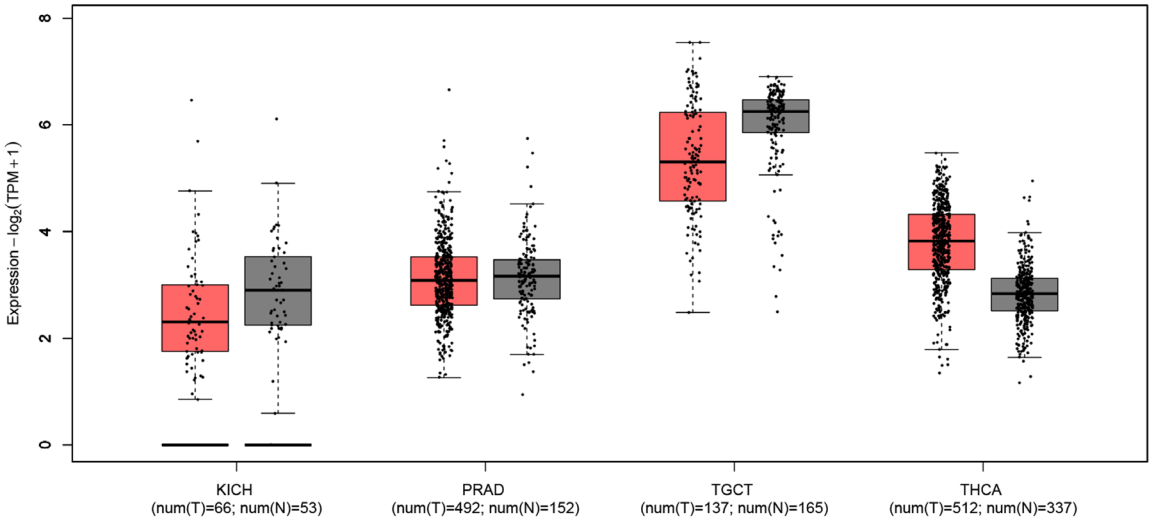

Supplementary Figure 2. TYMS expression showed no difference between KICH, PRAD, TGCT, or THCA and their comparable normal tissues. KICH, kidney chromophobe; PRAD, prostatic adenocarcinoma; TGCT, testicular germ cell tumors; THCA, thyroid carcinoma.

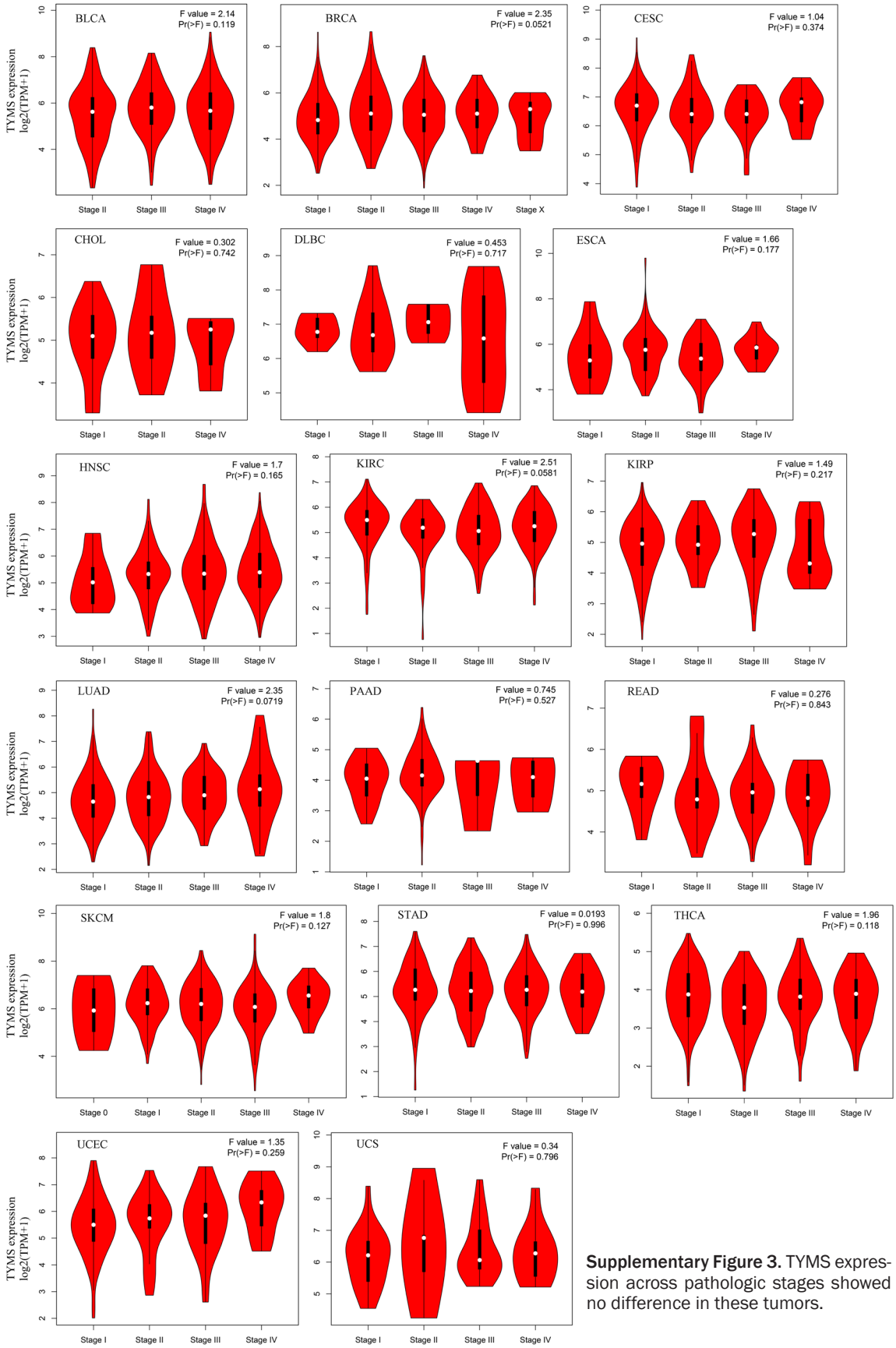

Supplementary Figure 3. TYMS expression across pathologic stages showed no difference in these tumors.

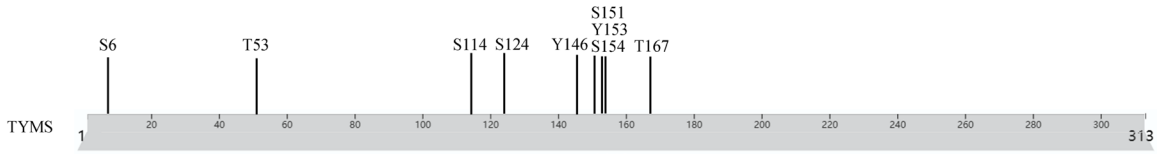

Supplementary Figure 4. Phosphoprotein site of TYMS showed in the axis.

Supplementary Figure 5. Correlation between TYMS and CD8+ immune cells (A) and NK cells (B). NK, natural killer.

Supplementary Table 2. Top 100 TYMS-correlated genes

Gene Symbol	Gene ID	Pearson correlation coefficient
NDC80	ENSG00000080986.12	0.73
EZH2	ENSG00000106462.10	0.66
NUSAP1	ENSG00000137804.12	0.66
WDR76	ENSG00000092470.11	0.65
MCM6	ENSG00000076003.4	0.65
KIFC1	ENSG00000237649.7	0.65
NCAPG	ENSG00000109805.9	0.64
KIF15	ENSG00000163808.16	0.64
LMNB1	ENSG00000113368.11	0.63
HMGB2	ENSG00000164104.11	0.63
FEN1	ENSG00000168496.3	0.63
PCNA	ENSG00000132646.10	0.63
GTSE1	ENSG00000075218.18	0.62
KIF2C	ENSG00000142945.12	0.62
MCM3	ENSG00000112118.17	0.61
PLK4	ENSG00000142731.10	0.61
CHAF1A	ENSG00000167670.15	0.61
CDC7	ENSG00000097046.12	0.61
CLSPN	ENSG00000092853.13	0.61
KIAA0101	ENSG00000166803.10	0.6
AURKB	ENSG00000178999.12	0.6
FANCI	ENSG00000140525.17	0.6
UHRF1	ENSG00000276043.4	0.6
FBXO5	ENSG00000112029.9	0.6
H2AFZ	ENSG00000164032.11	0.59
CENPU	ENSG00000151725.11	0.59
RAD54L	ENSG00000085999.11	0.59
NCAPG2	ENSG00000146918.19	0.59
DNMT1	ENSG00000130816.14	0.59
STMN1	ENSG00000117632.20	0.59
TMPO	ENSG00000120802.13	0.58
KIF4A	ENSG00000090889.11	0.58
PRC1	ENSG00000198901.13	0.58
NCAPH	ENSG00000121152.9	0.58
CENPK	ENSG00000123219.12	0.58
HMGN2	ENSG00000198830.10	0.58
ASPM	ENSG00000066279.16	0.58
KIF18B	ENSG00000186185.13	0.58
KIF11	ENSG00000138160.5	0.57
CHAF1B	ENSG00000159259.7	0.57
SKA1	ENSG00000154839.9	0.57
TCF19	ENSG00000137310.11	0.57
DONSON	ENSG00000159147.17	0.57
BUB1	ENSG00000169679.14	0.57
CCNB2	ENSG00000157456.7	0.57
CHEK1	ENSG00000149554.12	0.57
MCM2	ENSG00000073111.13	0.57
PSMC3IP	ENSG00000131470.14	0.57
SGOL2	ENSG00000163535.17	0.57

KIF23	ENSG00000137807.13	0.57
MCM5	ENSG00000100297.15	0.56
E2F1	ENSG00000101412.12	0.56
CDC45	ENSG00000093009.9	0.56
ASF1B	ENSG00000105011.8	0.56
CENPF	ENSG00000117724.12	0.56
CDCA5	ENSG00000146670.9	0.56
TUBA1B	ENSG00000123416.15	0.56
NUF2	ENSG00000143228.12	0.56
CDC25C	ENSG00000158402.18	0.56
CCNA2	ENSG00000145386.9	0.56
BRIP1	ENSG00000136492.8	0.56
MND1	ENSG00000121211.7	0.56
LRR1	ENSG00000165501.16	0.56
ZWINT	ENSG00000122952.16	0.56
TUBB	ENSG00000196230.12	0.55
CENPO	ENSG00000138092.10	0.55
SPC25	ENSG00000152253.8	0.55
POLA2	ENSG00000014138.8	0.55
H2AFV	ENSG00000105968.18	0.55
TPX2	ENSG00000088325.15	0.55
E2F2	ENSG00000007968.6	0.55
BIRC5	ENSG00000089685.14	0.55
SGOL1	ENSG00000129810.14	0.55
RFC2	ENSG00000049541.10	0.55
EXO1	ENSG00000174371.16	0.55
NEIL3	ENSG00000109674.3	0.55
EXOSC9	ENSG00000123737.12	0.55
PHF19	ENSG00000119403.13	0.55
FBXO43	ENSG00000156509.13	0.55
DLGAP5	ENSG00000126787.12	0.55
ZNF367	ENSG00000165244.6	0.55
KIF20A	ENSG00000112984.11	0.54
MXD3	ENSG00000213347.10	0.54
TIMELESS	ENSG00000111602.11	0.54
MAD2L1	ENSG00000164109.13	0.54
PRIM1	ENSG00000198056.13	0.54
CDT1	ENSG00000167513.8	0.54
UBE2T	ENSG00000077152.9	0.54
HJURP	ENSG00000123485.11	0.54
CKAP2L	ENSG00000169607.12	0.54
FAM64A	ENSG00000129195.15	0.54
FAM72B	ENSG00000188610.12	0.54
RNASEH2A	ENSG00000104889.4	0.54
GINS1	ENSG00000101003.9	0.54
METTL4	ENSG00000101574.14	0.53
NASP	ENSG00000132780.16	0.53
DTL	ENSG00000143476.17	0.53
RFC5	ENSG00000111445.13	0.53
TMPO-AS1	ENSG00000257167.2	0.53
DSN1	ENSG00000149636.15	0.53